Stabilization of superconductivity by magnetic field in out-of-equilibrium nanowires

Yu Chen, Yen-Hsiang Lin, S. D. Snyder, and A. M. Goldman
School of Physics and Astronomy, University of Minnesota, Minneapolis, Minnesota 55455, USA
(Received 3 February 2010; revised manuscript received 1 April 2010; published 14 February 2011)

A systematic study has been carried out on the previously reported "magnetic-field-induced superconductivity" of Zn nanowires. By varying parameters such as magnetic field orientation and wire length, the results provide evidence that the phenomenon is a nonequilibrium effect associated with the boundary electrodes. They also suggest there are two length scales involved, the superconducting coherence length and quasiparticle relaxation length. As wire lengths approach either of these length scales, the effect weakens. We demonstrate that it is appropriate to consider the effect to be a stabilization of superconductivity that has been suppressed by an applied current.

DOI: 10.1103/PhysRevB.83.054505 PACS number(s): 74.78.Na, 74.40.Gh, 74.25.F−, 74.25.Dw

I. INTRODUCTION

Superconducting nanowires have the potential for utilization in integrated circuits, as a consequence of their dissipationless nature. Upon scaling their sizes down below the coherence length, this characteristic can be lost due to the destruction of superconducting long-range order by either thermal or quantum fluctuations. Superconductors in this quasi-one-dimensional limit can have nonzero resistances produced by phase slip processes. This has been the focus of much research.[1–9]

Recently we reported on observations of "magnetic-field-enhanced superconductivity" in Zn nanowires.[10] In that article, we described lithographically made Zn nanowires with Zn electrodes, which, after being driven resistive by the current at low temperatures, were found to re-enter the superconducting state upon the application of small magnetic fields. In the following we report on experiments and analysis that go beyond the scope of the original article. We have varied the length and width of the nanowires as well as the magnetic field orientation with further analyses of the morphology of the samples and their critical currents. The results provide solid evidence not previously presented that the phenomenon is a nonequilibrium effect associated with the coupling to the boundary electrodes. In addition, it is appropriate to treat the effect as a *stabilization* or *recovery* of superconductivity, which was suppressed by the applied current. Although we do not present a formal theory to explain all of our results here, the effect is most likely a consequence of the dampening of phase fluctuations by quasiparticles which are created in the electrodes by small magnetic fields.

The superconductivity of nanowires may be significantly influenced by the state of their boundary electrodes. Because of the proximity effect, one would expect an enhancement of superconductivity when a wire is connected to superconducting electrodes, and a suppression when connected to normal electrodes. These manifest themselves as enhanced critical currents in superconducting microbridges[11] and suppressed critical temperatures in Al nanowires with Cu-coated Al electrodes.[12] In addition, theoretical studies have shown that a finite-length wire can undergo a superconductor-insulator transition through its coupling to the external environment.[13,14]

A recent study of electro-deposited Zn nanowires found that their coupling to bulk superconductors of other materials can cause the so-called "antiproximity effect".[15,16] In contrast with the usual proximity effect, at certain temperatures wires were found to enter the superconducting state from the normal state when the electrodes were driven normal by a magnetic field. Reproducing this effect in a different physical geometry was the motivation for the present investigation.

As described in detail in Ref. 10, samples in the configuration of a single Zn nanowire with wide Zn electrodes were prepared using a combination of multilayered photolithography, electron-beam lithography, and vapor deposition. The effect reported is robust and has been observed consistently in more than 20 samples including several made of Al instead of Zn (Ref. 17). In Table I, we list some key parameters for several representative samples. This includes the sample measured in Ref. 10, but here we will only discuss our latest results.

The paper is structured in the following manner. Experiments on the field-orientation dependence of the effect are presented in Sec. II. The wire length dependence is presented in Sec. III. Analysis of the granularity, critical field, and width dependence are presented in Sec. IV. Arguments that attribute the effect to the stabilization of superconductivity are contained in Sec. V. Section VI contains discussions of theories and conclusions.

II. FIELD ORIENTATION DEPENDENCE: BOUNDARY EFFECTS

We first consider the role of the boundary electrodes. To this end, measurements were carried out with different orientations of the applied field relative to the samples, both perpendicular to the wire and the plane of the substrate (the geometry used in the measurements in Ref. 10) and in the plane of the substrate and transverse to the wire see the insets of Figs. 1(b) and 1(c) .

The wire exhibits a wide transition region up to 900 Oe from the zero-resistance state to the normal state. This represents a two-step transition tuned by the magnetic field. As shown in Fig. 1(a), the first step of the transition actually corresponds to the magnetic field reaching the critical field of the electrodes. The height-to-width ratios are close to unity for the wire, but are only around 0.1 for the electrodes. As a consequence, when the field changes direction from perpendicular to transverse,

TABLE I. Parameters of representative samples. Wire widths and heights were determined by SEM and AFM, respectively. The transition temperature T_c was taken as the temperature of the half-normal resistance at a low applied current of 0.1 μA. The zero-temperature dirty limit coherence length was estimated as $\xi(0) \sim 0.855 \cdot (\xi_0 l_e)^{1/2}$, where ξ_0 is the BCS coherence length and l_e is the mean free path that is obtained from the product $\rho_{Zn} l_e = 2.2 \times 10^{-11}\ \Omega \cdot \mathrm{cm}^2$ at 4.2 K. The value of $\rho_{Zn} l_e$ used is from studies on single crystal Zn nanowires.[18] For the wires of finite lengths used in the current study, the conventional way of extracting the coherence length from $H_c(T)$ near T_c cannot be used due to complications associated with the alteration of the boundary conditions by the magnetic field. Also note that this may not be a good way to calculate these parameters for Sample H, but the results are given for completeness.

Sample	Width (nm)	Height (nm)	Length (μm)	T_c (K)	$\xi(0K)$ (μm)	ρ_{Zn}(4.2 K) ($\mu\Omega$-cm)	I_c(0 K) Theo. (μA)
A	85	150	1.5	0.85	0.22	11	120
B	80	90	1.5	0.83	0.19	14	56
C	60	100	1	0.76	0.25	8.4	53
D	60	100	2	0.76	0.26	7.8	55
E	60	100	4	0.76	0.28	6.3	61
F	60	75	10	0.76	0.22	11	35
G	65	100	1.5	0.78	0.27	6.9	66
H	500	175	1.5	0.81	0.46	2.5	1570

it is always effectively perpendicular to the wire. For the electrodes, the change of the field orientation is significant since the field goes from out of plane to in plane. The critical field of the electrodes increases by a factor of 5 when the magnetic field is switched from perpendicular to transverse, while the critical field of the wire basically remains unchanged as can be seen in Fig. 1(a). Note that this sample was brought to room temperature and attached to a different sample puck in the atmosphere in between the transverse and perpendicular measurements. This could be responsible for the slight change in the value of the wire's critical field at low current between the transverse and perpendicular curves in Fig. 1(a), or this change could be a reflection of the cross section of the wire not being a perfect square or circle.

For convenience we will represent data in the form of a resistance color contour map (RCCM) as in Figs. 1(b) and 1(c). The colors represent contours of constant resistance ranging from green (normal state resistance) to blue (zero resistance) with the other colors representing resistance values between these two according to the key next to the map. An ordinary superconducting RCCM would look like a dome, similar to Fig. 4. However the Zn nanowires have RCCM's which have a V-shaped structure at low magnetic fields and high currents. Note that we have used mostly RCCM's in the parameter space of magnetic field and current although they could just as easily be graphed in magnetic field and temperature space. We also will define three specific critical currents for the subsequent discussion. I_{c1} is the current where $R/R_n > 0.01$, which is where resistance first appears. I_{c2} is the critical current where $R/R_n < 0.99$, which is where resistance first begins to drop off from the normal state value, and finally, I_{c0} is the shoulder current for which a definition can be found in Ref. 10.

The RCCM of a 1.5 μm sample (Sample B) in the perpendicular magnetic field direction is shown in Fig. 1(b). In this RCCM, the regime of magnetic field enhanced superconductivity corresponds an increase in I_{c1} at low magnetic fields. Note that I_{c2} only decreases with the applied magnetic field and at relative low currents ($I \lesssim 3.0\,\mu$A), the wire does not exhibit any sign of an enhancement of superconductivity. The same qualitative behavior is easier to see in Fig. 1(c).

The blue contour is where the electrodes and wire are superconducting whereas the red contour is where the wire is superconducting and the electrodes are not because of the geometry. Therefore the boundary of these two contours is the critical field of the electrodes. The associated resistance originates from the proximity effect between the superconducting wire and the normal electrodes. Above this critical field, the system effectively becomes a NSN junction. The green region is where both the wire and electrodes are not superconducting. At low temperatures, the magnetic field between the green contour and red contour is roughly the critical field of the wire. One can plainly see that the re-entrance only occurs when the electrodes remain superconducting. This can be seen by comparing the critical field of the wire with the critical field of the electrodes.

Now, focusing on the enhancement regimes in the RCCM's shown in Figs. 1(b) and 1(c), one can immediately recognize the expansion of the regime of magnetic-field-enhanced superconductivity when the magnetic field is switched from perpendicular to transverse. In other words, a higher magnetic field is needed in the transverse direction to induce re-entrance into the superconducting state, compared with the perpendicular direction. Because the magnetic field remains perpendicular to the wire, this difference suggests that the observed enhancement of superconductivity is controlled by processes taking place in the electrodes in response to the applied magnetic field. However, what is unchanged is the amplitude of the enhancement, which can be taken as the increase of the critical current I_{c1}. This should be expected since the response of the wire to magnetic field is the same in both directions, and the field here is much smaller than the critical field of the wire itself.

III. WIRE LENGTH DEPENDENCE: TWO LENGTH SCALES

After establishing that the effect is associated with the boundary electrodes, we carried out measurements on wires of different lengths (Samples C: 4 μm, D: 2 μm and E: 1 μm). To minimize variations associated with fabrication, the wires were produced in the same process within a 100 μm square

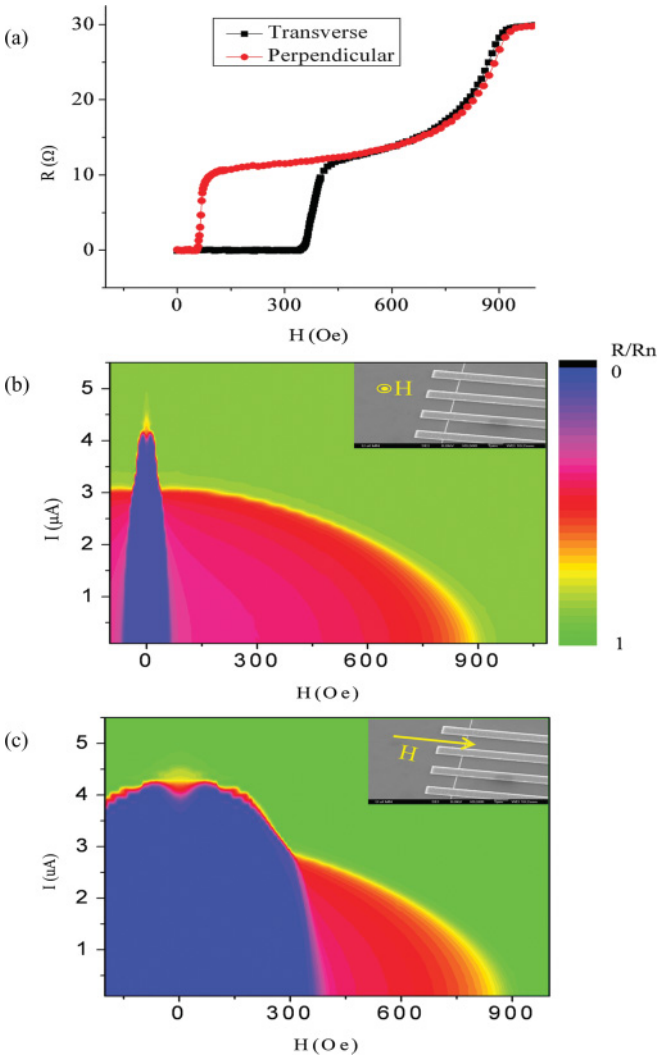

FIG. 1. (Color online) (a) Magnetoresistance of a 1.5-μm long wire (Sample B) with different field orientations, at a temperature 460 mK and with a current of 0.4 μA. (b) RCCM for this sample at 460 mK in a perpendicular field as indicated in the inset. (c) RCCM for this sample at 460 mK in a parallel field transverse to the axis of the wire as indicated in the inset.

on the same substrate. The RCCM's at 460 mK as a function of the current and magnetic field are shown for each wire in Fig. 2. By comparing the enhancement regimes of the three diagrams, the most remarkable feature is that longer wires exhibit a stronger effect, a larger increase of the critical current I_{c1}. This observation is seemingly counterintuitive since the enhancement effect has been shown to be a boundary effect. Naively thinking, the greater the distance to the boundaries, the less influence they should be expected to exert. One might therefore expect a longer wire to exhibit a weaker enhancement and eventually the effect should become negligible for an infinitely long wire.

Further measurements of an even longer wire (Sample F: 10 μm) helped to resolve this issue (this wire was prepared in a separate process and was thinner than Samples C, D, and E). In its RCCM at 460 mK, as shown in Fig. 3(a), the enhancement effect does seem to disappear. However, as 10 μm is still a finite length, the segments of the wire near the boundary electrodes should still be influenced by them, and therefore there should be some remnant of the enhancement effect in this wire. This can be seen by rescaling the RCCM; instead of having the colors ranging from 0 to R_n, a new RCCM has the color scale starting from 80% of the normal resistance, as shown in Fig. 3(b). Immediately, the enhancement can be recognized as the familiar V-shaped structure. However, this structure can no longer be understood as an increase of the lower critical current I_{c1}. Instead, it is a negative magnetoresistance that is only a small fraction of the zero field resistance.

Summarizing the various observations, it is clear that the enhancement effect becomes weaker in the short wire limit, but also becomes weaker in the long wire limit. The existence of these two limits strongly suggests that there are two characteristic length scales that determine the effect. As we will argue in Sec. V, these should be the superconducting coherence length and the quasiparticle relaxation length, two very important length scales for a superconducting system out of equilibrium.[19]

IV. WIRE WIDTH DEPENDENCE, GRANULARITY, AND CRITICAL CURRENT ANALYSIS

To better understand the origin of the enhancement we investigated the width dependence of the effect in two different

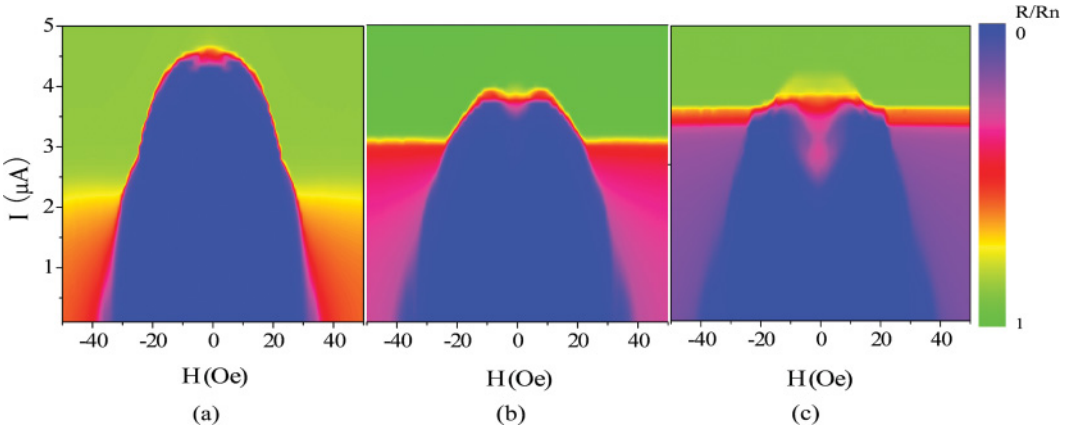

FIG. 2. (Color online) RCCMs at T = 460 mK, for wires of different lengths: (a) 1 μm, (b) 2 μm, and (c) 4 μm. (Samples C, D and E)

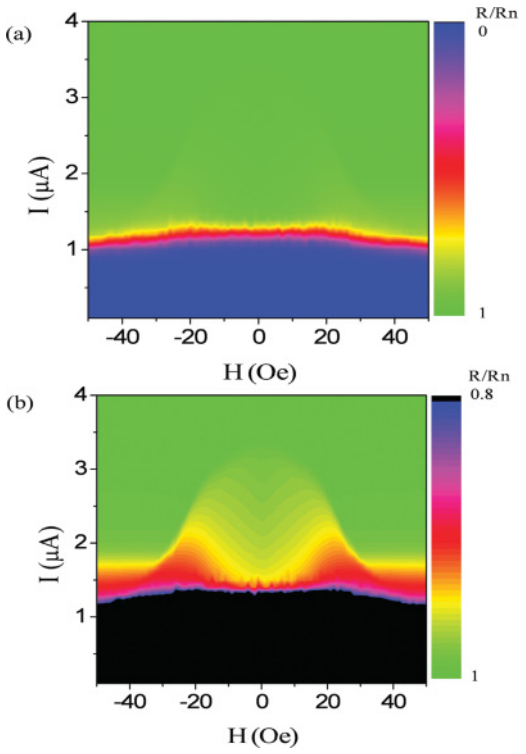

FIG. 3. (Color online) RCCM of a 10 μm long wire (Sample F) at 460 mK. The color scales as R/R_n: (a) from 0.1 to 1, and (b) from 0.8 to 1

ways, characterized the granularity of the nanowires, and analyzed the critical current as has been done in the past.[20] The first way we looked at the width dependence was by fabricating a 500-nm strip instead of a nanowire. The strip is wider than the coherence length but smaller than the electrodes. This should put it outside of the quasi-one-dimensional regime. As can be seen in Fig. 4, it showed no enhancement whatsoever. Its RCCM is the same as that of a bulk sample. There is not even a small negative magnetoresistance as was observed in the 10-μm long nanowire.

The second way we investigated the width dependence was through oxidation. Zinc readily oxidizes in air. In fact, this

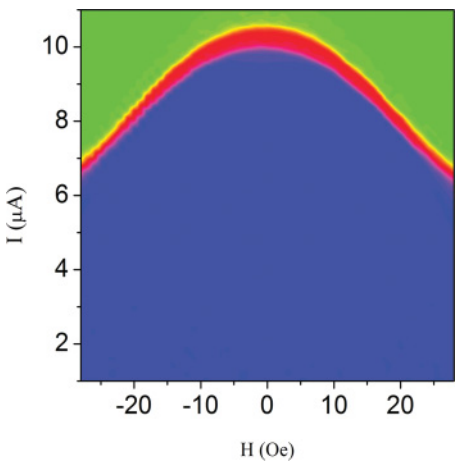

FIG. 4. (Color online) RCCM of a 500-nm wide Zn strip (Sample H). This is expected from a bulk sample.

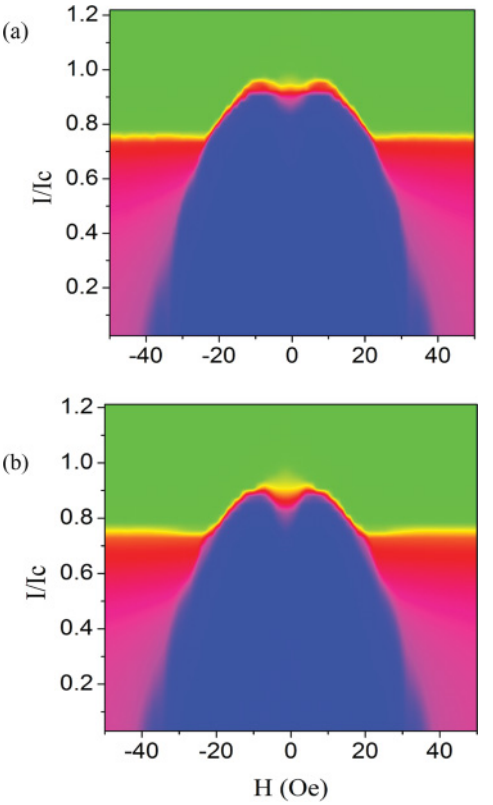

FIG. 5. (Color online) (a) Before prolonged exposure to air. (b) After exposure to air. The amount the critical current changes in the reentrant region has gotten slightly larger.

can be a hindrance to using the material as it does not oxidize just at the surface. The native oxide can penetrate quite deeply into a thin film, so we minimized the sample's exposure time to atmosphere for most samples.[10] However, we used this to our advantage by exposing a sample to the atmosphere after measuring it once. The resistance of the sample increased slightly after exposure to air for several days. If we assume that the resistance change is associated with the wire being thinner, then the wire was narrowed by ~10%. The sample showed a slightly larger effect, as can be seen in Fig. 5, meaning that the difference between the highest value of I_{c1} and the lowest value has increased slightly. However, it is not enough to be fully conclusive, and subsequent attempts to oxidize samples proved fruitless because samples left in air for too long were no longer conductive and the structural characterization of the wires usually destroyed them.

Using the scanning electron microscope (SEM) images taken during characterization, such as Fig. 6(a), it can be seen that the wires are granular. The grain size is approximately the same size as the wire width and height in all SEM images. Several atomic force microscope (AFM) scans confirm that the wires are indeed rough and granular with a grain size approximately the size of the nanowire. This could lead to the wires behaving as one-dimensional arrays of Josephson junctions. Although nanowires have been treated in this manner theoretically,[21] the precise problem considered here has not been discussed. While granularity certainly is relevant, its role in our observations remains unclear.

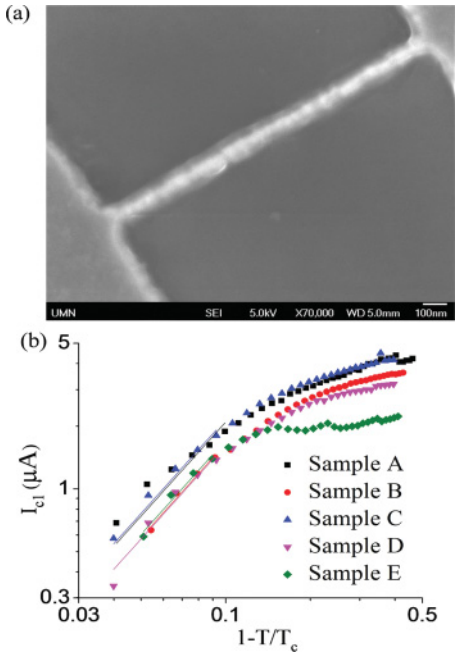

FIG. 6. (Color online) (a) SEM image of Sample A, granularity is apparent from this picture. (b) Log-log plot of the critical current (I_{c1}) vs. temperature which is fit by the GL theory (1) when $T/T_c > 0.9$. The adjusted coefficient of determination for each sample is A = 0.827, B = 0.986, C = 0.967, D = 0.968, and E = 0.973.

At low temperatures, the current-driven transition of the wire is broad, associated with the three currents defined previously. I_{c1} is plotted as a function of temperature in Fig. 6(b). As one can see, there is agreement between the behavior of I_{c1} and the prediction of the Ginsburg-Landau (GL) theory, Eq. (1), for points with $T/T_c > 0.9$, but not over the entire temperature range[19]

$$j_c = j_c(0)\left(1 - \frac{T}{T_c}\right)^{3/2}. \quad (1)$$

However, there is no agreement between this data and the Bardeen expression

$$j_c = j_c(0)\left[1 - \left(\frac{T}{T_c}\right)^2\right]^{3/2}, \quad (2)$$

or the Kupriyanov-Lukichev theory over the entire temperature window available.[20,22,23] Note that I_{c1} is suppressed relative to either of these predictions and that the transition in the R versus I curves is quite sharp near T_c, which makes I_{c1}, I_{c0}, and I_{c2} almost indistinguishable. An attempt to extract the temperature dependence of I_{c0} has been much more difficult as it is harder to define, especially near T_c.

In addition, I_{c1}, I_{c0}, and I_{c2} deviate strongly from the theoretically predicted GL critical pair-breaking current density for isolated superconducting wires (see Table I)[20]

$$j_c(0) = \frac{8\pi^2\sqrt{2\pi}}{21\zeta(3)e}\left[\frac{(k_B T_c)^3}{\hbar v_f \rho_{Zn}(\rho_{Zn} l_e)}\right]^{1/2}. \quad (3)$$

A part of the deviation may be associated with utilizing parameters such as the Fermi velocity of the free electron model. Also, wire granularity could lead to a system of high disorder as shown in Fig. 6(a). This could explain the low critical currents.[19] Another explanation could be the oxidation layer at the surface of the nanowires, which could make the cross sectional area smaller than that inferred from AFM and SEM measurements. Finally, perhaps quantum confinement could explain it, but it is all just speculation at this point.

V. SUPPRESSION AND STABILIZATION OF SUPERCONDUCTIVITY

After reviewing the experimental observations, there is a fundamental question that needs to be addressed: Is this effect an enhancement of superconductivity by a magnetic field? It has been demonstrated that applying a small magnetic field can cause an increase in the values of currents at which the wire leaves its zero resistance state. According to conventional theories of superconductivity, these currents and temperatures directly relate to the amplitude of the order parameter.[19] So does applying a magnetic field increase the amplitude of the order parameter? The answer can be obtained by re-examining the RCCM's of wires of different lengths, shown in Fig. 2. As mentioned previously, these wires were made in the same fabrication process and on the same substrate. Therefore they are expected to have the same amplitude of the order parameter when at the same temperature, current, and magnetic field. Having the superconducting boundaries included, one would expect the previous argument to be valid only for wires exceeding the superconducting coherence length ξ since it is the characteristic length scale of the proximity effect. For this reason, we temporarily exclude the 1 μm wire from the discussion since its length is on the order of twice the coherence length.

A comparison of the RCCM's of the 4 and the 2 μm sample can be made. We first consider the values of I_{c1} in a zero field. They are $\sim$3.5 μA for the 2 μm wire and $\sim$2.5 μA for the 4 μm wire, a difference of approximately 40%. On the other hand, if one compares the maximum value of I_{c1} in a small magnetic field, one can see that the two wires share almost the same value $\sim$3.7 μA. This is more evident from a similar comparison of the critical temperatures T_{c1} at which wires leave the zero resistance state at 2.5 μA (see Fig. 7). Once again, one can see that the maximum values of T_{c1} are almost the same $\sim$0.65 K for both wires, but in the zero field T_{c1} differs by $\sim$40% ($T_{c1} \sim 0.64$ K for the 2 μm wire and $T_{c1} \sim 0.46$ K for the 4 μm wire).

With this in mind, it is therefore more appropriate to treat the effect in two steps. First, superconductivity, or more accurately the zero resistance state of the wire, is suppressed in zero magnetic field by the applied current. Second, a small magnetic field can induce a *recovery* or *stabilization* of the suppressed superconductivity.

It is therefore useful to examine the RCCM's for these three wires in the zero field, shown in Fig. 8. The suppression is exhibited as broadened transition regions, where a longer wire would be expected to have a stronger "enhancement" effect since it would exhibit a stronger suppression by the current in the zero field, Fig. 8. A similar argument applies to differences between the diagrams in Fig. 7 for the increase of T_{c1} at 2.5 μA in fields.

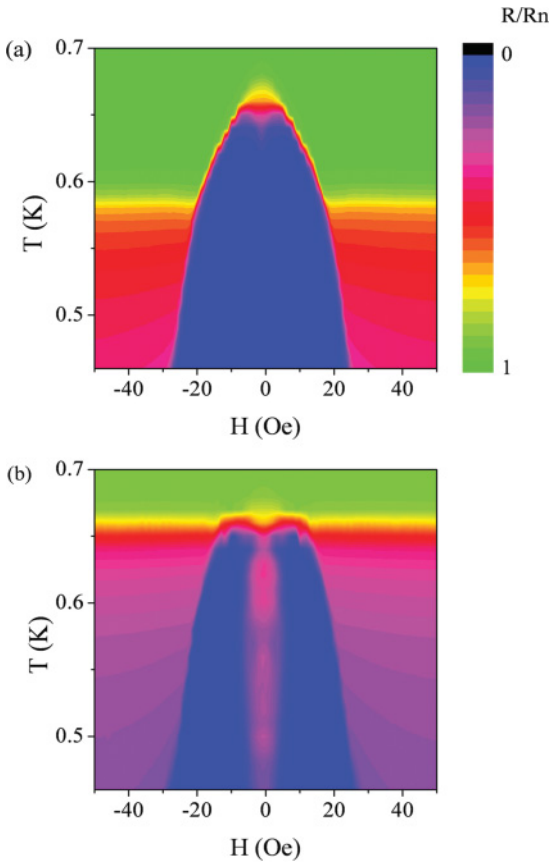

FIG. 7. (Color online) RCCM's at a current of 2.5 μA of wires of different lengths: (a) $L = 2\,\mu$m and (b) $L = 4\,\mu$m (Samples D and E).

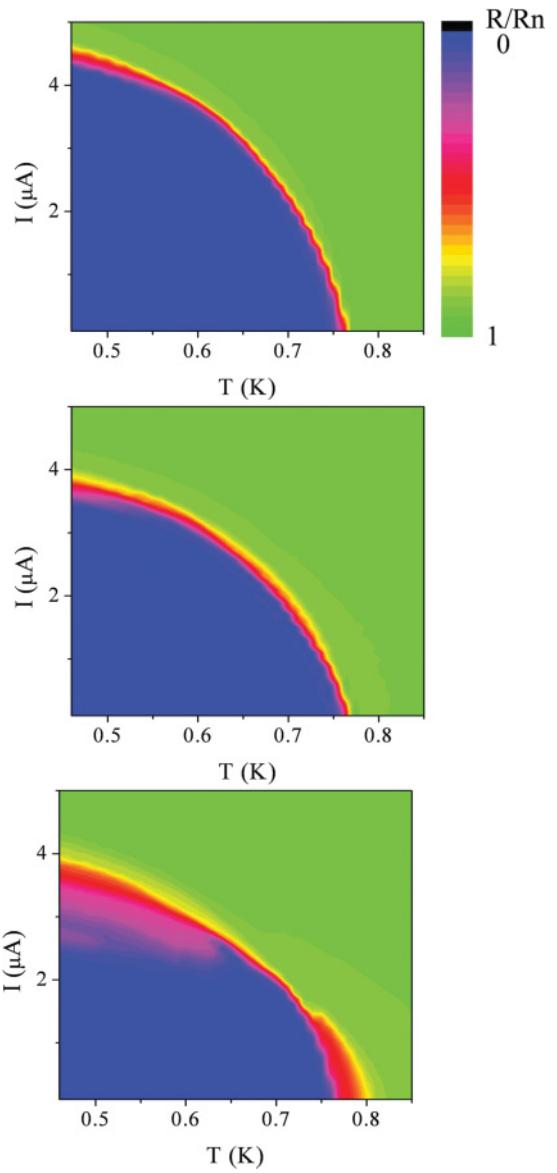

FIG. 8. (Color online) RCCM's at zero field for wires of different lengths (a) 1 μm, (b) 2 μm, and (c) 4 μm (Samples C, D, and E).

VI. DISCUSSION AND CONCLUSION

Before discussing the potential physical mechanism, we must first address the important experimental issue of heating. At high currents, heating has been known to strongly modify the transition of superconducting wires. The consequence of heating is that a hot spot will be formed quenching the superconductivityy of the wire.[24,25] In the case of heating, the *I-V* curves are expected to be hysteretic. However, in the present study, both the current and magnetic field driven transitions are reversible without any hysteresis. It indicates that the samples are not only in the overdamped regime, but also are sufficiently cooled by their electrical connections and the substrate. This is possibly associated with the fact that the cross sectional areas are relatively large and resistances small in the samples.

In addition, we exclude the possibility that the magnetic-field-stabilized superconductivity comes from the enhanced thermal conductivity of both the wire and the electrodes in the magnetic field because different parts of the transition regime respond to magnetic field differently. This exclusion and others have been discussed in detail in Ref. 10.

Even though it is evident that the observed effect is a recovery of suppressed superconductivity, its actual physical mechanism remains unclear. In the following, we will present some qualitative explanations. First, we consider the suppression of the superconductivity of the wire. Now a superconducting wire with nonzero order parameter can acquire a nonzero resistance through several mechanisms. The first one is associated with the penetration of the electric field when the wire is connected to normal electrodes. This mechanism apparently does not apply here since the electrodes remain superconducting over the whole range of re-entrance, as discussed in Sec. II.

The second mechanism is associated with the formation of phase slip centers. A theory of the current-driven superconducting transition in quasi-one-dimensional wires was developed by Kramer and Baratoff.[26] Their numerical calculations, based on the time-dependent GL equations, demonstrated this transition is associated with two currents $I_{\rm min}$ and $I_{\rm max}$. For $I < I_{\rm min}$, the superconducting state is stable. For $I > I_{\rm max}$, the normal state is stable. For $I_{\rm min} < I < I_{\rm max}$, the system remains superconducting while becoming resistive due to phase slip processes. Since $I_{\rm max}$ can be roughly taken as the depairing current, this calculation suggests that

quasi-one-dimensional superconductors can be resistive at currents lower than the depairing current. This qualitatively resembles the suppression of superconductivity discussed here, with $I_{\min}$ and $I_{\max}$ corresponding to I_{c1} and I_{c2}.

For wires of lengths less than the quasiparticle relaxation length and connected to superconducting electrodes, the location of the phase slip center would most likely be at the midpoint of the wire. The observation that shorter wires have a weaker suppression can therefore be explained as coming from their superconductivity being more strongly supported, or the phase slip processes being more strongly suppressed, by the superconducting boundaries. This has been treated in a theoretical study of the conditions for the occurrence of phase slip centers.[27] The critical current j_{c1} at which phase slips start to occur is obtained by comparing the relaxation rates of the amplitude and phase of the order parameter. With superconducting boundaries

$$j_{c1} \sim j_o \coth(L/2\Lambda_Q). \tag{4}$$

Here Λ_Q is the quasiparticle relaxation length and $j_0 = c\Phi_0/8\pi^2\Lambda^2\xi$ (the GL critical current $\sim 0.385 j_0$). One therefore can see that j_{c1} decreases until saturating when the wire length exceeds a certain value. For wires of lengths approaching the coherence length, it is more appropriate to treat the system as an S-c-S junction (S stands for superconductor, c stands for constriction). In this case, the system will have a higher critical current since it now can withstand a higher phase gradient $\sim 1/L$ instead of $\sim 1/\xi$ for longer wires. This has been observed as a high critical current for the 1 μm wire in our study, as shown in Fig. 2(a).[19]

The second issue to address is how suppressed superconductivity can be recovered by an applied magnetic field. Existing models have been discussed in Ref. 10. Here we will focus on two models that consider the reduction of Λ_Q and the dissipation dampening of phase slips.[28–30]

Λ_Q is known to decrease in a magnetic field.[31] Theoretical studies have shown that this reduction can effectively lead to "enhancements" of superconductivity in one dimension, either as a negative magnetoresistance[28] or as an increase of the critical current.[29] In particular, the critical current j_{c1} has been predicted to increase in a small magnetic field due to the reduction of Λ_Q, and it is especially pronounced for weak superconductors such as Al and Zn. Larger fields, on the other hand, will lead to a decrease of j_{c1} due to the reduction of the order parameter.[29] This prediction is in qualitative agreement with our observations, but problems still exist when applying the model to the experimental results. The discussion of Λ_Q only considers its variation with the field due to changes of the wire's order parameter. In contrast, the field orientation dependence of the observed effect demonstrates that the superconducting boundary electrodes play a major role. In addition, the model is based on the time-dependent GL equation, which is only valid near T_c.

It has been suggested recently that the small magnetic fields used here cannot appreciably change the value of Λ_Q. However, this does not rule out the possibility of changes in the order parameter in the leads being the cause of the effect. When the order parameter in the electrodes is suppressed, the flux of quasiparticles diffusing into the wire can become greater. This could help explain the results seen here and should be pursued further.[32]

The wire resistance in the transition regime below I_{c0} is associated with phase slips driven by fluctuations. However, the nature of these fluctuations is unclear. Numerical fits of various models of the temperature dependence of the wire resistance have been carried out. In the low current limit, reasonable fits of thermal activated phase slip models can be obtained[2,3]

$$R = R_Q \frac{\hbar\Omega(T)}{k_B T} e^{-\Delta F(T)/k_B T}. \tag{5}$$

Here, $R_Q = h/4e^2$ is the quantum resistance for Cooper pairs, $\Omega(T)$ is the attempt frequency, and ΔF is the energy cost of nucleating a phase slip

$$\Omega(T) = \frac{L}{\xi(T)} \left(\frac{\Delta F(T)}{k_B T}\right)^{1/2} \frac{8k_B(T_c - T)}{\pi\hbar}, \tag{6}$$

$$\Delta F(T) = \frac{8\sqrt{2}}{3} \frac{H_C^2(T)}{8\pi} A\xi(T), \tag{7}$$

where $H_c(T)$ is the thermodynamic critical field and $\xi(T)$ is the GL coherence length. At high currents the broadening of the transition is such that all the existing models, including those that treat quantum phase slips (QPS's)[4,5] fail to fit the data. This does not exclude the possibility of QPS's.

Figure 9 shows a zero-field RCCM of a 1.5 μm wire (Sample G), with I_{c0} labeled as the white line. It is clear that the transition region between I_{c1} and I_{c0} becomes more pronounced at lower temperature and persists toward zero temperature. As thermal fluctuations are negligible in this temperature range, the result suggests that the phase slips might be driven by quantum fluctuations, even though the data cannot fit by existing QPS models.

If the resistance seen in the transition region is driven by QPS's, the field-enhanced superconductivity could be explained by the interplay between QPS's and the dissipation associated with quasiparticles generated by a magnetic field. Theories of the interplay between dissipation and QPS's in superconducting nanowires have been presented.[5,21,30]

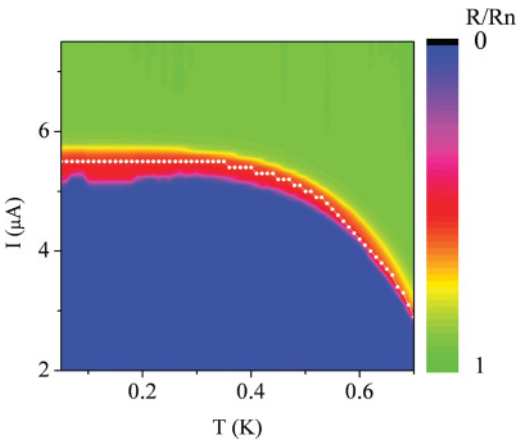

FIG. 9. (Color online) RCCM of a 1.5 μm wire (Sample G) in zero field, with the temperature range extended down to 50 mK. The white line labels the position of the shoulder in R-I curves.

These exploit analogies between nanowires and Josephson junctions.[33,34] Dissipation can dampen QPS's and therefore stabilize superconducting long-range order.

For a wire connected to electrodes, theoretical studies have shown that dissipation from the external environment can also dampen phase slips.[13,14] When a magnetic field is applied, it will affect both the phase slips and the dissipation. The applied magnetic field suppresses the order parameter and increases the rate of QPS's, increasing the wire resistance.[30] On the other hand, it will enhance the dissipation with an increased density of quasiparticles. This increase can be exponentially large at low temperatures compared with the power-law change of the QPS rate, which could give negative magnetoresistance in the low field.

With all of this in mind, a qualitative scenario can be constructed. Increasing the current results in phase slip generation, which broadens the resistive transition. When a magnetic field is applied, quasiparticles are produced in the electrodes. These quasiparticles dampen the phase slip processes that produce resistance by increasing the dissipation, resulting in the wire recovering its zero resistance state.

To conclude, when the wire length is short, with a length on the order of the superconducting coherence length, the *suppression* of superconductivity by the applied current is weak. In this case, the superconductivity of the wire is strongly supported by the superconducting electrodes. The Cooper pairs can easily propagate coherently over the whole length of the wire and phase slips are rare. When the wire length approaches or exceeds the quasiparticle relaxation length, the *stabilization* of superconductivity by magnetic field is weak. In this case, quasiparticles from the electrodes need to diffuse a long distance to reach the phase slip center—the midpoint of the wire. As a consequence there is a high probability for them to be converted into Cooper pairs. The effect of quasiparticles in dampening phase slip processes is therefore limited. This is why the observed effect is weak when the wire is too short or too long. The recovery of superconductivity is strongest for wires of intermediate lengths, shorter than the quasiparticle relaxation length, but longer than the coherence length.

Although the above is a phenomenological explanation of the effect, it is developed from a set of inferences based on experimental observations and theories not specific to the detailed experimental configuration. A formal theory that can be compared in detail with the experimental results would be needed to fully understand the observed phenomena.

ACKNOWLEDGMENTS

The authors thank Alex Kamenev for useful discussions. This work was supported by the U.S. Department of Energy under Grant No. DE-FG02- 02ER46004 and by the National Science Foundation under Grant No. NSF/DMR-0854752. Part of this work was carried out at the University of Minnesota Characterization Facility and the Nanofabrication Center, which receive partial support from the NSF through the NNIN program.

[1] W. A. Little, Phys. Rev. **156**, 396 (1967).
[2] J. S. Langer and V. Ambegaokar, Phys. Rev. **164**, 498 (1967).
[3] D. E. McCumber and B. I. Halperin, Phys. Rev. B **1**, 1054 (1970).
[4] N. Giordano, Phys. Rev. Lett. **61**, 2137 (1988).
[5] A. D. Zaikin, D. S. Golubev, A. van Otterlo, and G. T. Zimanyi, Phys. Rev. Lett. **78**, 1552 (1997).
[6] R. S. Newbower, M. R. Beasley, and M. Tinkham, Phys. Rev. B **5**, 864 (1972).
[7] C. N. Lau, N. Markovic, M. Bockrath, A. Bezryadin, and M. Tinkham, Phys. Rev. Lett. **87**, 217003 (2001).
[8] M. Zgirski, K.-P. Riikonen, V. Touboltsev, and K. Arutyunov, Nano Lett. **5**, 1029 (2005).
[9] F. Altomare, A. M. Chang, M. R. Melloch, Y. Hong, and C. W. Tu, Phys. Rev. Lett. **97**, 017001 (2006).
[10] Y. Chen, S. D. Snyder, and A. M. Goldman, Phys. Rev. Lett. **103**, 127002 (2009).
[11] M. Octavio, W. J. Skocpol, and M. Tinkham, Phys. Rev. B **17**, 159 (1978).
[12] G. R. Boogaard, A. H. Verbruggen, W. Belzig, and T. M. Klapwijk, Phys. Rev. B **69**, 220503 (2004).
[13] H. P. Buchler, V. B. Geshkenbein, and G. Blatter, Phys. Rev. Lett. **92**, 067007 (2004).
[14] H. C. Fu, A. Seidel, J. Clarke, and D.-H. Lee, Phys. Rev. Lett. **96**, 157005 (2006).
[15] M. Tian, N. Kumar, S. Xu, J. Wang, J. S. Kurtz, and M. H. W. Chan, Phys. Rev. Lett. **95**, 076802 (2005).
[16] M. Tian, N. Kumar, J. Wang, S. Xu, and M. H. W. Chan, Phys. Rev. B **74**, 014515 (2006).
[17] See supplemental material at [http://link.aps.org/supplemental/10.1103/PhysRevB.83.054505] for an example of Al data.
[18] U. Schulz R. Tidecks, J. Low Temp. Phys. **71**, 151 (1988); B. N. Aleksandrov, Sov. Phys. JETP **16**, 286 (1963).
[19] M. Tinkham, *Introduction to Superconductivity*, 2nd ed. (Dover, New York, 1996).
[20] J. Romijn, T. M. Klapwijk, M. J. Renne, and J. E. Mooij, Phys. Rev. B **26**, 3648 (1982).
[21] G. Refael, E. Demler, Y. Oreg, and D. S. Fisher, Phys. Rev. B **75**, 014522 (2007).
[22] J. Bardeen, Rev. Mod. Phys. **34**, 667 (1962).
[23] M. Yu. Kupriyanov and V. F. Lukichev, Sov. Phys. JETP **67**, 1163 (1988).
[24] W. J. Skocpol, M. R. Beasley, and M. Tinkham, J. Appl. Phys. **45**, 4054 (1974).
[25] M. Tinkham, J. U. Free, C. N. Lau, and N. Markovic, Phys. Rev. B **68**, 134515 (2003).
[26] L. Kramer and A. Baratoff, Phys. Rev. Lett. **38**, 518 (1977).
[27] S. Michotte, S. Matefi-Tempfli, L. Piraux, D. Y. Vodolazov, and F. M. Peeters, Phys. Rev. B **69**, 094512 (2004).
[28] K. Arutyunov, Physica C: Superconductivity **468**, 272 (2008).
[29] D. Y. Vodolazov, Phys. Rev. B **75**, 184517 (2007).
[30] A. D. Zaikin, D. S. Golubev, A. van Otterlo, and G. T. Zimanyi, Phys. Usp. **41**, 226 (1998).
[31] J. Clarke, in *Nonequilibrium Superconductivity, Phonons, and Kapitza Boundaries*, edited by K. E. Gray (Plenum, New York, 1981).
[32] D. Y. Vodolazov and F. M. Peeters, Phys. Rev. B **81**, 184521 (2010).
[33] S. Chakravarty, Phys. Rev. Lett. **49**, 681 (1982).
[34] A. Schmid, Phys. Rev. Lett. **51**, 1506 (1983).